

# An analytical model for simulating the bond of prestressed concrete during the prestressed force release

J.M. Benítez & J.C. Gálvez

*Universidad Politécnica de Madrid, Madrid, Spain*

**ABSTRACT:** A bond analytical model is proposed in this paper. The model is capable of reproducing the bond stress developed between the steel and concrete, in precast prestressed elements, during the entire process of prestressing force release. The bond stress developed in the transmission zone, where the bond stress is not constant, is also obtained. The steel and concrete stresses as well as the slip between both materials can be also estimated by means of the relation established in the model between these parameters and the bond stress. The model is validated with the results of a series of tests, considering different steel indentation depths and concrete covers and it is extended to evaluate the transmission length. This has been checked by comparing the transmission length predicted by the model and one measured experimentally in two series of tests.

## 1 INTRODUCTION

Precast prestressed concrete elements are widely used for construction in Europe. Hollow core slabs and prestressed joists are profusely used for concrete structures in building construction. In both cases, the effectiveness of prestressing force is based on the bond between steel (wire or strand) and concrete.

The mechanisms that contribute to bond between prestressing steel and surrounding concrete are chemical adhesion, friction and mechanical interlocking between wire indentations and concrete (Janey 1954).

The interlock mechanism found between the steel and concrete during the prestressed force release may be explained through an analogous mechanism such as that proposed by Tepfers (Tepfers 1973, Tepfers & Olsson 1992) for bars on the reinforced concrete (see Figure 1). When the prestressing force of steel is released at the end of the element by cutting the wire, it tends to pierce in the concrete and develops tangential stress (bond stress) and radial stresses at the interface between the steel and concrete. Both stresses may be related by means of the  $\alpha$  angle (see Figure 1). The typical value of  $\alpha$  for ribbed bars is  $45^\circ$  (Cairns & Johns 1995), though there is no proposal for indented prestressed wires or strands.

In the case of indented wires, the wedging action generated by Poisson's effect is magnified by the indentations on the surface of the wire, increasing the tension ring (Gambarova & Rosati 1996, Abrishami

& Mitchell 1992, Gustavson 2004, den Uijl 1992a). Moreover, Hoyer's effect, presents on the ends of the prestressed concrete structural elements, is directly related with Poisson's effect (FIB 2000). These aspects are beneficial for bond, though they may be harmful if concrete splits, dropping the confinement and diminishing the bond (Gálvez et al. 2009, Abrishami & Mitchell 1992, den Uijl 1992b, Benítez 2006).

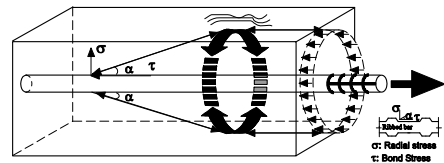


Figure 1. Bond behaviour of deformed bars, radial component of the bond stresses balanced by tensile stress in the uncracked ring of concrete.

On the other hand, a frequent problem of the precast industry is to evaluate the real transmission length in precast prestressed concrete structural elements. The semi-empirical formulae proposed by codes are usually thought for conventional concrete and usual cast conditions, but high performance concrete (high-strength, self-compacting, etc.) and non-usual cast conditions (v.gr. accelerated curing processes) are becoming more and more frequent. In these cases experimental measurement is needed, though the standardised methods are expensive and so difficult to apply by industry. Analytical and numerical mod-

els, based on parameters measured experimentally with tests being simpler than complete transmission length tests, would be welcomed. This paper presents an analytical model for steel-concrete bonding when the prestressing force is transmitted by releasing the steel (wire or strand). The model is based on Tepfer's proposal for reinforced concrete (Tepfers 1973, Tepfers & Olsson 1992) and on the work of van der Veen 1991, who modelled the thick-walled concrete ring to predict the cracking of the concrete on a cross-section for a known radial stress, not considering any effect of Poisson's ratio. For a practical application of the model, extension has taken place to evaluate the transmission length. The model is validated with the results of two experimental series of transmission length evaluation and good agreement was reached. These results corroborate the possibility of extending the analytical model of the previous phase from wires to strands.

## 2 THEORETICAL APPROACH

The prestressing process of the precast prestressed concrete elements includes two consecutive steps: a) steel wire prestressing, and b) prestressing force transmission after an accelerated curing process of concrete (Figure 2). Bond between wire and concrete during force releasing process can be analytically expressed as follows.

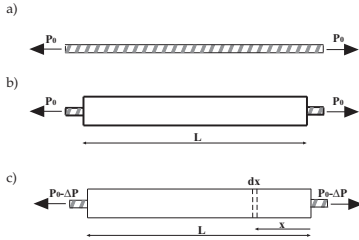


Figure 2. Manufacturing process of the prestressed concrete prism: a) alone prestressed wire, b) wire with cast concrete before prestressing force release, c) prestressing force release.

It is considered a slice of a prismatic structural element with a  $dx$  thickness, placed at a distance  $x$  from one of the prism end (Figure 2.c). Equilibrium of forces in the axis prism direction (see Figure 3) leads to the following differential equation:

$$\frac{\partial \Delta \sigma_x}{\partial x} = - \frac{p_e}{A_s} \tau \quad (1)$$

where  $\Delta \sigma_x$  is the wire stress variation between sections  $x$  and  $x+dx$  (at  $x=0$ ,  $\Delta \sigma_{x=0} = \Delta \sigma_0 = \Delta P/A_s$ ),  $p_e$  is the wire perimeter,  $A_s$  is the area of wire section and  $\tau$  is the mean tangential stress between wire and concrete in the slice.

The slip between wire and concrete at any section may be expressed, based on the difference between the strains of both materials, as follows:

$$\frac{ds}{dx} = \frac{\Delta \sigma_x}{E_s} - \frac{\sigma_c}{E_c} \quad (2)$$

where  $s$  is the slip between wire and concrete,  $dx$  is the slice thickness,  $E_s$  and  $E_c$  are Young's modulus of the steel and concrete, respectively, and  $\sigma_c$  is the concrete normal stress at  $x$  section.

The concrete stress in the section placed to an  $x$  distance from the prism end can be calculated establishing the equilibrium of the forces depicted in Figure 4, where  $\sigma_0$  is the wire initial stress, that is to say  $P_0/A_s$ , and  $\Delta \sigma_0$  is the stress released at the wire end ( $x=0$ ), that is  $\Delta P/A_s$ . The following equation is obtained from this equilibrium:

$$\sigma_c = \frac{A_s}{A_c} (\Delta \sigma_0 - \Delta \sigma_x) \quad (3)$$

$A_c$  is the net area of the concrete section (gross area minus area of wire).

$\Delta \sigma_x$  is found by replacing equation (3) into equation (2). Integrating equation (2), along  $x$  distance, the slip  $s$  at every section is found.

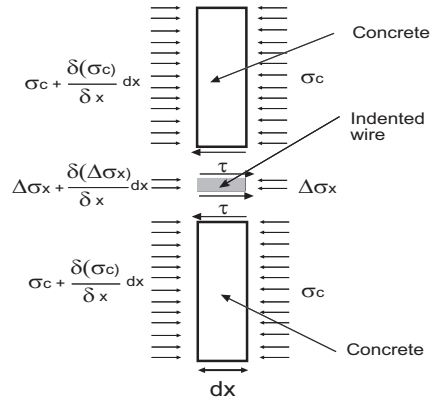


Figure 3. Balance of stresses in a slice of  $dx$  thickness.

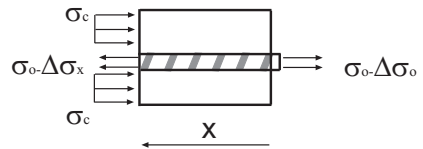


Figure 4. Balance of forces in a part of the specimen with  $x$  length, measured from the end.

The differential equation (1) can be calculated taking into account the concrete confinement of the wire. For such a purpose, the analogy of a thick-walled cylinder is adopted. Figure 5 shows the sketch of the model.  $R_1$  is the inner radius (the radius of the wire) and  $R_2$  is the outer radius (minimum distance from wire axis to the external face of the concrete prism in the transversal direction). So that  $R_2 - R_1$  is the minimum concrete cover of the wire in the prism.

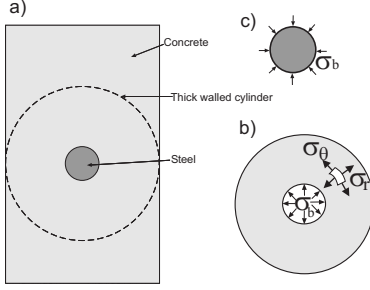


Figure 5. Interaction between concrete and steel at the interface: a) thick-walled cylinder approach of the prism cross section, b) stresses in concrete, c) stresses in steel due to confinement.

Hereinafter, a linear elastic behavior of the materials is adopted, with it also being assumed that there is no cracking of concrete. According to Figure 5,  $\sigma_\theta$  and  $\sigma_r$  are, respectively, the circumferential and the radial stresses at any internal point of the thick-walled cylinder cross section.

Equal circumferential strain at steel-concrete interface for both materials is assumed, giving equation 4 (for more details see Benítez & Gálvez 2011):

$$\sigma_b = J \Delta \sigma_x - M \Delta \sigma_0$$

$$\text{with } \begin{cases} J = \frac{\nu_s E_c + \frac{A_s}{A_c} \nu_c E_s}{(1 - \nu_s) E_c + (H + \nu_c) E_s} \\ M = \frac{\nu_c E_s \frac{A_s}{A_c}}{(1 - \nu_s) E_c + (H + \nu_c) E_s} \end{cases} \quad (4)$$

where  $H = (R_2^2 + R_1^2) / (R_2^2 - R_1^2)$ ,  $J$  and  $M$  are dimensionless parameters that depend only on the geometry and mechanical properties of the materials.

Taking into account the Tepfer's equation (5) and replacing it into equation (1) considering (4) (see equation (6)), the differential equation (7) is obtained:

$$\tau = \sigma_b \cot \alpha \quad (5)$$

$$\tau = B_1 \Delta \sigma_x - B_2 \Delta \sigma_0$$

$$\text{with } \begin{cases} B_1 = \frac{J}{\tan \alpha} \\ B_2 = \frac{M}{\tan \alpha} \end{cases} \quad (6)$$

$$\frac{\partial \Delta \sigma_x}{\partial x} = -B \Delta \sigma_x + C$$

$$\text{with } \begin{cases} B = \frac{p_e}{A_s} B_1 \\ C = \frac{p_e}{A_s} B_2 \Delta \sigma_0 \end{cases} \quad (7)$$

where  $k$  is an integration constant to be determined for each particular case.

For every concrete prism section, the tangential stress developed between steel and concrete grows during the process of prestressing force release up to a certain value,  $\tau_{max}$ , that cannot be exceeded. In this work it is assumed, for sake of simplicity, that once this critical value has been reached the tangential stress remains constant and equal to  $\tau_{max}$ . Nevertheless, adoption of a lower residual value would not present any significant difficulty.

### 3 BOND STRESS-SLIP CALCULATION

To calculate  $\Delta \sigma_x$  value, as a function of  $x$ , it is needed to know if the tangential stress has reached the critical value  $\tau_{max}$  at any section. In case that it happens, it is needed to know the value of  $x$  along which the  $\tau$  stress has exceeded the  $\tau_{max}$ . This value of  $x$  is noted as  $X_{LIM}$ . According to this aspect, integration of the equation (2) distinguishes two cases:

#### 3.1 Tangential stress is lower than $\tau_{max}$ at any value of $x$ ( $X_{LIM} = 0$ )

For  $x = 0$   $\Delta \sigma_x = \Delta \sigma_0$ , equation (8) may be expressed as follows:

$$\Delta \sigma_x = \Delta \sigma_0 \left( \frac{B_2}{B_1} + \left( 1 - \frac{B_2}{B_1} \right) e^{-Bx} \right) \quad (9)$$

Replacing equation (9) in (3) the normal stress in concrete is:

$$\sigma_c = \frac{A_s}{A_c} \left( 1 - \left( \frac{B_2}{B_1} + \left( 1 - \frac{B_2}{B_1} \right) e^{-Bx} \right) \right) \Delta \sigma_0 \quad (10)$$

Equations (9) and (10) allows to solve the differential equation (2).

In our particular case, a prism with an  $L$  length and symmetrically released force from both ends, the integration of equation (2) leads to:

$$s = \Delta \sigma_0 A_s \left( \beta \left( \frac{B_2 L}{B_1} - \frac{B_2 - B_1}{B_1} \frac{1 - e^{-\frac{BL}{2}}}{B} \right) - \frac{L}{2} \frac{1}{A_c E_c} \right)$$

$$\text{with } \beta = \frac{A_c E_c + A_s E_s}{A_c E_c A_s E_s} \quad (11)$$

For this prestressed concrete prism, the tangential stress between  $x=0$  and  $x=L/2$  is obtained from equation (6) and expressed as

$$\tau = \Delta \sigma_0 B_1 \left( 1 - \frac{B_2}{B_1} \right) e^{-Bx} \quad (12)$$

### 3.2 Tangential stress reaches $\tau_{max}$ inside $x$ distance ( $X_{LIM} > 0$ )

Based on the analytical solution, the  $\tau$  value given by equation (12) may be larger than  $\tau_{max}$ , the result is clearly not acceptable. According to the aforementioned hypothesis, the tangential stress between the steel and concrete is assumed to be constant and equal to  $\tau_{max}$  in the segment  $0 \leq x \leq X_{LIM}$ .  $X_{LIM}$  is variable since it depends on the released force, growing during the process. The integration of the equation (1) may be easily carried out with  $\tau = \tau_{max}$  and  $\Delta\sigma_{x=0} = \Delta\sigma_0$ , obtaining the value of  $\Delta\sigma_x$  in this segment ( $0 \leq x \leq X_{LIM}$ ):

$$\Delta\sigma_x = -\frac{p_e}{A_s} \tau_{max} x + \Delta\sigma_0 \quad (13)$$

In order to determine the stresses distribution along the prism the  $X_{LIM}$  value should be known. The  $X_{LIM}$  value is found from equations (13) and (6) producing  $x = X_{LIM}$ .

The first condition consists on imposing the same value of  $\Delta\sigma$  en  $x=X_{LIM}$ , considering the corresponding equations, (13) and (8), leading to:

$$\Delta\sigma_{x=X_{LIM}} = -\frac{p_e}{A_s} \tau_{max} X_{LIM} + \Delta\sigma_0 = \frac{C}{B} \Delta\sigma_0 + k e^{-B X_{LIM}} \quad (14)$$

the second leads to (15) by replacing equation (8) in (6) and particularized for  $x = X_{LIM}$

$$\tau_{max} = B_1 k e^{-B X_{LIM}} \quad (15)$$

giving eventually:

$$X_{LIM} = \frac{A_s}{p_e \tau_{max}} \left( \left( 1 - \frac{B_2}{B_1} \right) \Delta\sigma_0 - \frac{\tau_{max}}{B_1} \right) \quad (16)$$

$$k = \frac{\tau_{max}}{B_1} e^{\frac{B_1 - B_2}{\tau_{max}} \Delta\sigma_0 - 1} \quad (17)$$

Replacing  $k$  in equations (8) and (5),  $\Delta\sigma_x$  and  $\tau$  are expressed for  $x \geq X_{LIM}$  as:

$$\Delta\sigma_x = \frac{B_2}{B_1} \Delta\sigma_0 + \frac{\tau_{max}}{B_1} e^{\frac{B_1 - B_2}{\tau_{max}} \Delta\sigma_0 - 1 - B x} \quad (18)$$

$$\tau = \tau_{max} e^{\frac{B_1 - B_2}{\tau_{max}} \Delta\sigma_0 - 1 - B x}$$

To determine the slip steel-concrete along the prism, the differential equation (2) is integrated, distinguishing two zones  $0 \leq x \leq X_{LIM}$  and  $x \geq X_{LIM}$  obtaining:

$$0 \leq x \leq X_{LIM}$$

$$s = \frac{((B_2 - B_1) \Delta\sigma_0 + \tau_{max}) (\beta E_s A_s (\Delta\sigma_0 (B_2 - B_1) + \tau_{max}) + 2 \Delta\sigma_0 B_1)}{2 E_s B \tau_{max} B_1} \quad (19)$$

$$x \geq X_{LIM}$$

$$s = \left( A_s \Delta\sigma_0 \frac{B_2}{B_1} \beta - \frac{A_s \Delta\sigma_0}{E_c E_c} \right) \left( \frac{L}{2} - X_{LIM} \right) - \frac{\tau_{max} \beta A_s}{B_1 B} \left( e^{\left( \frac{B_1 - B_2}{\tau_{max}} \Delta\sigma_0 - 1 - \frac{B L}{2} \right)} - e^{\left( \frac{B_1 - B_2}{\tau_{max}} \Delta\sigma_0 - 1 - B X_{LIM} \right)} \right) \quad (20)$$

## 4 MODEL VALIDATION

The proposed analytical model is validated with the experimental results published by Galvez et al. 2009. The test procedure was based on releasing, under control displacement, the prestressing force of a single wire embedded in a concrete prism. The slip between steel and concrete at the end of the specimen was recorded throughout the whole test. Figure 6 shows the geometry and the dimensions of the specimens.

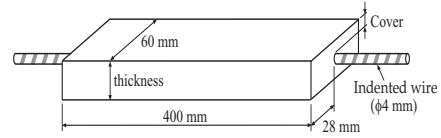


Figure 6. Geometry and dimensions of the specimens form Galvez et al. 2009.

Three concrete covers and three indentation depths of the wire were studied. In this work the experimental results corresponding to the larger covers were the only ones adopted, the reason being guarantee of an appropriate confinement of the wire and avoidance of radial concrete cracking. Table 1 shows the indentation depth of the wire. The estimated angle  $\alpha$  is also included in Table 1. The maximum tangential stress at steel-concrete interface has been got experimentally (Benítez 2006), by means of a push-in test with small thickness specimen, and it is shown in the Table 1.

Table 1. Indented wires indentations depth,  $\alpha$  angle and maximum bond stress at interface.

Denomination	Indentation Depth (mm)	$\alpha$ (°)	Maximum bond stress (MPa)
Smaller	0.01-0.02	80	2.28
Medium	0.04-0.06	77	2.28
Larger	0.1-0.11	70	3.16

Figure 7 compares model prediction and experimental results of the slip between wire and concrete at the end of the specimen versus prestressed force released, for specimens with 2.25φ(9mm) concrete cover and medium kindentations depth. Figure 8 shows analogous results for specimens with 3.25φ

(13mm) concrete cover. Similar behavior is found in the rest of the specimens (see Benítez and Gálvez 2011).

In the case of the specimens with smaller concrete cover (Figure 7), the model prediction is a sufficiently accurate approximation of the experimental results, even though it tends to overvalue the slip. In the case of the specimens with larger cover (Figure 8) the modelling fits better in the scatter band. The most accurate model prediction of Figure 8, specimens with larger concrete cover, is understood because larger concrete cover leads to a higher confinement of the wire, being more consistent with the hypothesis of a thick-walled cylinder for the cross-section.

## 5 TRANSMISSION LENGTH CALCULATION

The proposed analytical model may be used to evaluate the transmission length when the concrete is not cracked and the prestressed steel (wire or strand) confined inside the concrete element.

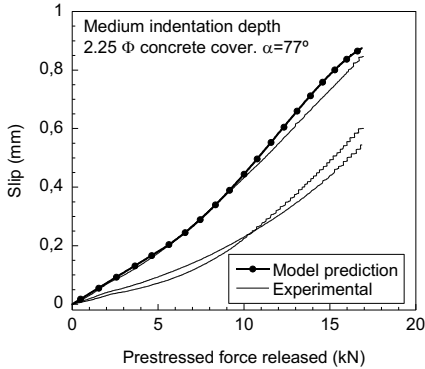


Figure 7. Experimental results (Gálvez et al. 2009) and model prediction of the prestressed force release versus slip. Specimen manufactured with 2.25 $\Phi$  and medium indentation depth.

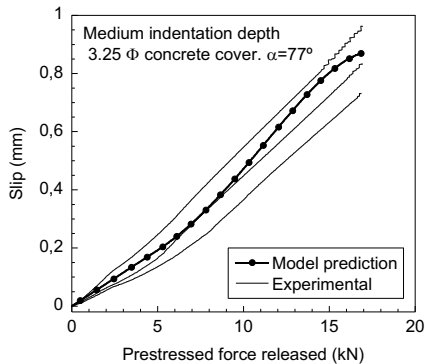


Figure 8. Experimental results (Gálvez et al. 2009) and model prediction of the prestressed force release versus slip. Specimen manufactured with 3.25 $\Phi$  and medium indentation depth.

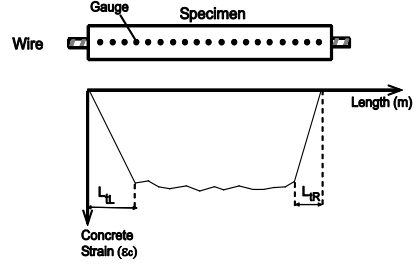


Figure 9. Measurement of the bond length from concrete deformations

The evaluation of the transmission length is based on the concrete strain along the specimen, see Figure 9, which can be calculated easily by dividing the equation (3) by Young's Modulus of the concrete,  $E_c$ , and taking into account equations (9), (13) and (18). Since the analytical model provides the strain of the concrete along the specimen, this model is used to evaluate the transmission length.

To validate the model for determining the transmission length, the results of two different experimental programs were analytically simulated.

The first of them was carried out by Russell & Burns 1997, who manufactured pretensioned prisms of 102mm x 127mm x 3,660mm with seven-wire strands. They used two different single strands: 12.7mm and 15.2mm strand diameter, placed in the barycentre of the cross-section. The material properties were:  $E = 27$  GPa,  $f_{ct} = 28$  MPa and  $\nu = 0.2$ , for concrete; and  $E = 194$  GPa and  $\nu = 0.3$ , for steel. Young's Modulus of concrete was estimated according to Model Code specifications. The force released was that corresponding with a steel stress of 1,396 MPa. With regard to the interface parameters, the critical tangential strength was  $\tau_{max} = 4.0$  MPa, according to the Model Code,

$$\tau_{max} = \eta_{p1} \eta_{p2} f_{ctd} = 1.2 \times 1.0 \times 3.3 = 4.0 \text{ MPa} \quad (21)$$

where  $\eta_{p1}$  and  $\eta_{p2}$  are parameters fixed by Model Code ( $\eta_{p1}$  takes into account the type of prestressing tendon and  $\eta_{p2}$  the position of the tendon) and  $f_{ctd}$  is the lower design tensile strength. The considered  $\alpha$  angle was  $\alpha = 10^\circ$ , fixed for the best fit of the numerical prediction.

Figures 10 show the results for 12.7mm and 15.2mm strand diameters, respectively, where  $L_t$  is the transmission length. The experimental results may be approximated by two linear branches. As figures show, the analytical model properly fit the experimental results. Concrete strains along the specimen and transmission length are accurately predicted by the proposed model. The second series of experimental results are the tests carried out by Oh & Kim 2001 who manufactured single strand pretensioned prisms of 115.2 x 200 x 3,000mm<sup>3</sup>, with a seven-wire strand with a diameter of 12.7mm.

In this series the wire was out of the centroid of the cross-section. The only materials parameter known is the compression concrete strength at the releasing moment,  $f_{ci} = 46.7$  MPa. Other parameters have been estimated according to this data and the Model Code prescriptions, and were:  $E = 30$  GPa and  $\nu = 0,2$ , for concrete; and  $E = 194$  GPa and  $\nu = 0,3$ , for steel.

The force released was that corresponding with a steel stress of 1,500 MPa, while the critical tangential stress at interface was  $\tau_{max} = 6$  MPa, according to the Model Code (see equation 26). The  $\alpha$  angle adopted is  $\alpha = 10^\circ$ .

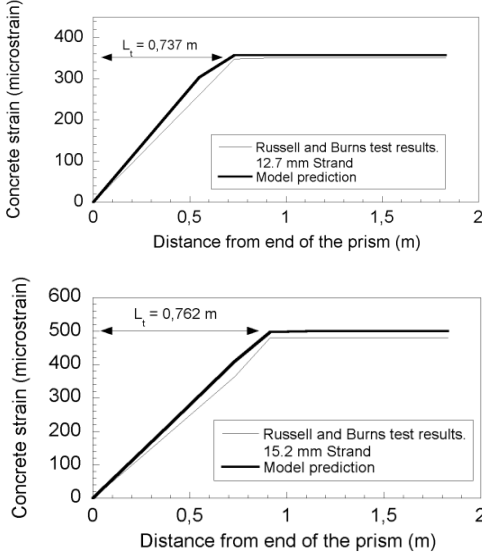


Figure 10. Strain profile and transmission length. Comparison of model with experimental results from Russell & Burns 1997 (12.7mm and 15.2 seven-wire strand specimens).

Contemplating the eccentricity of the steel, equation (3) is modified to equation (22)

$$\sigma_c = (\Delta\sigma_0 - \Delta\sigma_x) \frac{A_s}{A_c} + \frac{(\Delta\sigma_0 - \Delta\sigma_x) A_s e^2}{I} \quad (22)$$

where  $e$  is the load eccentricity and  $I$  is the cross-section moment of inertia.

Figure 11 compares the experimental results from the Oh and Kim test and the analytical prediction. As can be seen, the model is consistent with the transfer length and accurately predicts the concrete strain.

The rotation of the strand during the sliding is not directly incorporated in the model, but is indirectly included by the fitting of the maximum tangential stress and  $\alpha$  angle, affected by the strand rotation. The study of the influence of the rotation of the strand in the transmission length is beyond the scope of this paper.

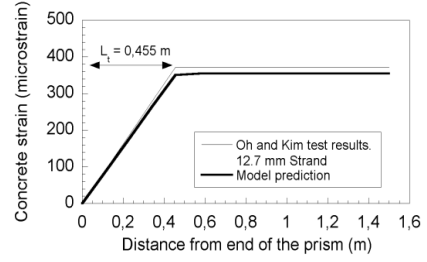


Figure 11. Strain profile and transmission length. Comparison of model with experimental results from Oh & Kim 2001 (12.7mm seven-wire strand specimens).

The transmission length proposed by the Model Code for a pretensioned tendon is:

$$l_{bpt} = \alpha_8 \alpha_9 \alpha_{10} l_{bp} \frac{\sigma_{pi}}{f_{pd}} \quad (23)$$

with

$\alpha_8$  gradual release 1.0, sudden release 1.25

$\alpha_9$  moment and shear verification 1.0,  
tensile stresses in anchorage zone 0.5

$\alpha_{10}$  strand 0.5, indented wire 0.7

$l_{bp}$  basic anchorage length

$\sigma_{pi}$  steel stress after release

$f_{pd}$  design strength of tendon

As can be checked, the experimental results and the model prediction of the transmission length of the tests performed by Russell & Burns 1997 and Oh & Kim 2001 properly fit with the value calculated with equation (23).

Equation 23 leads to estimated values of the transmission length based on extensive experimental tests. Analogous equations are proposed by ACI 318 and Eurocode 2.

The model proposed in this paper does not try to substitute these useful standard models, especially in the engineering design field. In many design codes the experimental approach to evaluating the transmission length is allowed and recommended, especially with non-conventional concretes and new materials, or treatments of the steel surface. In such cases, the experimental evaluation of the transmission length is expensive and requires several series of tests. The proposed model may help to evaluate the transmission length, or even the anchorage length, based on simpler and cheaper tests, reducing the number of transmission length tests. Moreover, the model assists in providing knowledge of the distribution of the tangential and normal stresses, between concrete and steel, in the transmission length zone.

## 6 CONCLUSIONS AND FINAL COMMENTS

An analytical model to evaluate the steel-concrete interaction in prestressed concrete elements during the prestressing force release has been proposed. The model evaluates the tangential and normal stresses in steel-concrete interface along the whole length of the element and is based on parameters with physical meaning and those that are experimentally measurable. The model has the advantage of including the Poisson ratio in the evaluation of confinement steel, as well as bond stress along the structural element. It should be noted that concrete splitting has not been taken into account. The model is suitable for confined steel in structural elements where there is no radial cracking of the concrete. The proposed model has been extended to evaluate the transmission length of pretensioned seven-wire strands in prestressing concrete specimens. Two series of experimental tests were used to validate the analytical modelling of the transmission length.

Based on these results, the proposed analytical model may help to the experimental evaluation of the transmission length. The relationship between bond and slip, obtained from a test simpler than complete transmission length test, may be used to estimate the transmission length. Moreover, a parametric study may be performed, based on the results of an individual transmission length test, and even different bond steel-concrete conditions may be considered in this transmission length evaluation.

## ACKNOWLEDGEMENTS

The authors gratefully acknowledge the financial support for the research provided by the Spanish Ministerio de Ciencia e Innovación under grant DPI2011-24876 and IPT-42000-2010-31.

## REFERENCES

- Abrishami, H. & Mitchell, D. 1992. Simulation of uniform bond stress. *ACI Materials Journal*. 89; No. 2; 161-168.
- Benítez, J.M. & Gálvez, J.C. 2011. Bond modelling of prestressed concrete during the prestressing force release. *Materials and Structures*. 44:263-278.
- Benítez, J.M. 2006. Estudio de la interacción entre el alambre preteso y el hormigón durante la transmisión de la fuerza de pretensado. Ph. D. Thesis.
- Cairns, J. & Johns, K. 1995. The splitting forces generated by bond. *Magazine of Concrete Research*. 47; 153-165.
- FIB 2000. Bond of reinforcement in concrete. State of art report task group Bond Models. FIB bulletin 2000, 10.
- Gálvez, J.C., Benítez, J.M., Tork, B., Casati, M.J. & Cendón, D.A. 2009. Splitting failure of precast prestressed concrete during the release of prestressing force. *Engineering Failure Analysis*, 16: 2618-2634.
- Gambarova, P.G. & Rosati, G.P. 1996. Bond and splitting in reinforced concrete: test results on bar pull-out. *Materials and Structures*. 29, 267-276.
- Gambarova, P.G., Rosati, G.P. & Zasso, B. 1989. Steel-to-concrete bond after concrete splitting: Constitutive laws and interface deterioration. *Materials and Structures*; 22(131):347-356.
- Gustavson, R. 2004. Experimental studies of the bond response of three-wire strands and some influencing parameters. *Materials and Structures*. 37: 96-106.
- Janney, J.R. 1954. Nature of bond in pretensioned prestressed concrete. *ACI J.* 25 (9): 717-736.
- Oh, B.H. & Kim, E.S. 2001. Realistic evaluation of transfer lengths in pretensioned, prestressed concrete members. *ACI Structural Journal*. 97; 6: 821-830.
- Russell, B.W. & Burns, N.H. 1997. Measurement of transfer lengths on pretensioned concrete elements. *Journal of Structural Engineering*. 123; 5: 541-549.
- Tepfers, R. 1973. A theory of bond applied to overlapped tensile reinforcement slices for deformed bars. Chalmers University of Technology. Division of Concrete Structures. Göteborg, Sweden; publication 73:2.
- Tepfers, R. & Olsson, P.Å. 1992. Ring test for evaluation of bond properties of reinforcing bars. In: *Bond in Concrete: From Research to Practice*. Riga Technical University and CEB. Latvia, Riga. 1; 1:89-99.
- den Ujil, J.A. 1992a. Bond and splitting action of prestressed strand. *Bond in Concrete: From Research to Practice*, Riga Technical University and CEB, Latvia, Riga. 1; 2:79-88.
- den Ujil, J.A. 1992b. Bond and splitting action of prestressed strand. *Bond in Concrete: From Research to Practice*, Riga Technical University and CEB, Latvia, Riga, 1992. 1; 2:79-88.
- van der Veen, C. 1991. Splitting failure of reinforced concrete at various temperatures. *Fracture Processes in Concrete, Rock and Ceramics*. J.G.M. van Mier, J.G. Rots and A. Baker: RILEM.